Slovenian Veterinary Research
DOI 10.26873/SVR-1694-2023
UDC 599.742.71:616.12-089:616-089.853:303.824
Pages: 57–71

Case Report

Clinical and Diagnostic Imaging Findings in a Bengal Tiger (*Panthera tigris tigris*) With Craniocervical Artery Dissection: A Case Report

Key words

Bergeyella zoohelcum;
ischemic stroke;
subarachnoid haemorrhage;
tiger;
transient ischemic attack

Peyman Mohammad Zadeh[1]*, Nilufar Shadan[2], Sajjad Mohammadi[3], Fatemeh Najafi[3], Aida Bashiri[4]

[1]Department of Pathobiology, Sanandaj Branch, Islamic Azad University, Sanandaj, Iran, [2]Islamic Azad University, Shahrekord Branch, Shahrekord, Iran, [3]Islamic Azad University, Sanandaj Branch, Sanandaj, Iran, [4]Razi University, Kermanshah, Iran

***Corresponding author:** peymanpathologist@iausdj.ac.ir

Abstract: This study aims to examine different aspects of Craniocervical Artery Dissections, which resulted in the animal's death following a sequence of pathological events. Following the physical damage to the female Siberian tiger neck due to the Agonistic behaviour of the male tiger, diagnostic tests such as complete medical examination, Time-of-Flight (TOF) MRA imaging and radiography, as well as sampling for clinical assessment, haematology, microbial culture, and antibiogram was performed, initial treatment was prescribed, and PCR was performed. Unfortunately, the Medical treatment measures were inadequate, and the animal died. Therefore, necropsy, histopathological examination, and immunohistochemistry staining were performed. The results of the microbiological study included the identification of *Bergeyella zoohelcum* for the first time in this animal species, as well as diagnostic findings; necropsy and histological examinations, including aneurysm, subarachnoid haemorrhage, and ischemic stroke, were provided as well as Horner's intramural hematoma and rupture of the carotid arteries and internal jugular vein, which has never been described before. Whole-body trauma computed tomography with an adapted scanning protocol for the craniocervical vessels is a safe, fast, and feasible method for detecting vascular injuries. It allows prompt further treatment if necessary. This method could be a part of a broad screening protocol for craniocervical vessels in documented injuries of the head and neck and trauma mechanisms influencing the craniocervical region as well.

Received: 28 January 2023
Accepted: 5 July 2023

Introduction

The Royal Bengal Tiger belongs to the Feliformia suborder of the Carnivora order consisting of "cat-like" carnivorans. He belongs to a subspecies of *Panthera tigris tigris* that is exclusive to The Middle East and India (1). The white tiger, also known as the bleached tiger, is a pigmentation variant (leucistic) variety of Royal Bengal Tigers, Amur tigers, and a Crossbreed hybrid of the two that are occasionally seen in the wild in Indian states (2,3). Tigers are globally listed as "Endangered" on the International Union for the Conservation of Nature (IUCN) Red List of Threatened Species (4). The Malayan and Sumatran sub-species are listed as "Critically Endangered." Intraspecific lethal encounters, Illegal hunting, habitat degradation, and fragmentation are all threats to this species, which is expected to have less than 3890 wild individuals by the end of 2023. (5). Thus, Examining different life-threatening factors and the pattern of causing injuries in each can directly benefit Wildlife survival biologists and wildlife veterinarians (6). Among these life-threatening factors, the pattern and type of injuries in fatal encounters due to conflict remain unknown. Tigers have lethal encounters with each other for access to Hunting resources, mates, and parental care. The most important reasons for interference between tigers in the wild include: Fighting over territory because they are solitary and maintaining individual territories. Next is Fighting over mates because tigers have a Polygyny mating system. As

a result, this characteristic leads to competition between males for access to females. Also, Infanticide and cannibalism are seen in felines, including tigers. Mortality caused by Hostile male tigers can affect Proportionate regional distribution, demography, and reproductive success. Finally, the last item is, Sibling rivalry; whenever a female tiger has two offspring at once, there is the potential for sibling rivalry. Tiger's Sibling rivalry is aggressive and can result in siblicide. Nevertheless, in zoos, the fundamental causes of conflicts between tigers include human errors, accidental access to nearby shelters, behavioural and neurological problems such as zoochosis, and aggressive and stereotypic behaviour due to captivity. The chance to experience positive social interactions and mating are vital for captive tigers. However, if this experience is not managed and happens accidentally, it often leads to unfortunate results, and in most cases, it will lead to death. The result is often clear regardless of the reason for these deadly conflicts. Severe pathological injuries often lead to damage to the vital organs of the neck, multiple cranial lacerations, fractures, traumatic amputations, persistent neurological deficits and fracture-dislocation of cervical vertebrae, abrasions, and crushes secondary to the dragging of the victim's body.

This case report outlines the multiple sources of injury and pathology that can result from such an attack. The discussion focuses on the injury pattern seen in large feline attacks. We present a rare fatal case of a tiger attack on another tiger during the night hours while the male entered the female cage. These two tigers had a five-year-long relationship with each other, and the discovery of his death astonished the zoo administration. This case describes the necropsy findings emphasizing the distribution of injuries and the histopathological findings. The details of the Histopathological injury pattern and radiological findings have been discussed.

Materials and methods

Case presentation

A brutal fight between two tigers took place due to sexual coercion following the access of a male Bengal tiger (*Panthera tigris tigris*) to the night enclosure of a white Siberian tiger (*Amur tiger*) at the Eram Zoo in Tehran, Iran. After entering, the male tiger violently tries to mate (After being informed that the zoo keepers saw them in a sexual position), but the female did not allow it due to oestrus problems. As a result, the male tiger violently bites the neck of the female tiger later, and after being informed, the zoo keepers separate the two tigers. Initial treatment immediately began with taking the necessary measures, including irrigation of the affected area using sterile saline to reduce bacterial load. After 10 hours, and due to the symptoms of pain and restlessness, the animal was anaesthetized using a combination of Ketamine Hydrochloride (Bremer Pharma GMBH, 34414 Warburg, Germany) and Medetomidine Hydrochloride (Laboratorios syva s.a.u, Avda. Parroco Pablo Diez, 49-5724010 Leon, Spain) (K: 2.3mg/kg+M:0.9 mg/kg IM; antagonized by 0.23mg/kg IM Atipamezole (Laboratorios syva s.a.u, Avda. Parroco Pablo Diez, 49-5724010 Leon, Spain).

Clinical examinations and diagnostic imaging

During anaesthesia, the gross examination was performed; A thorough examination of the animal initially began with signalling and a complete description of the animal, including species, breed, age, gender, reproductive status, and other distinguishing characteristics were noted. Further, history, including environment, diet, medical history, fertility history, vaccination status, and current status, were evaluated. Hydration status is further expressed as a percentage of body weight (0-15%), which can be somewhat subjective, and it is reported as "adequate," "marginal," or "inadequate," which was insufficiently observed in the case of this animal. Next, the vital signs were checked, which included (a body weight of 215.3 kg) and a temperature (of 40.6, which is the usual range in tigers 37.8-39.4). Then, the rectal area was checked for signs of diarrhoea, parasites, and other abnormalities. The heart/pulse rate (56 to 97 bpm) was (109 bpm). Evaluation of pulse rate, strength, and quality was done in the form of thread. The next item was Respiratory rate and character with a typical range (8.4 ± 3.6), which was 10.3 in this tiger. Then the perfusion indices were checked, which included Mucous membrane colour (MM) and Capillary refill time (CRT), which was prolonged CRT (> 2 seconds) (Table1). The next step was the head and neck evaluation (EENT/Oral) which both sides of the face and head were checked for symmetry. Assess eyes for size, position, discharge – lids, conjunctiva, sclera, pupil, cornea, lens note discharge, inflammation, redness, uneven/abnormal pupil size, corneal clouding, squinting. The nose was evaluated and nares for symmetry, conformation, and evidence of discharge. The oral cavity was examined - lips, mucous membranes, teeth, hard and soft palate, tongue, pharynx, and tonsils. Carriage and position of ears were evaluated, and thickness/malleability of pinnae and cleanliness of ear canals, submandibular lymph nodes, and salivary glands (normally palpable) were palpated. The following parameter was Trunk and Limbs (INTEG, M/S, PLN) evaluation. The body for symmetry, masses, and tenderness was Inspected. Each limb and joint was palpated, and abnormalities in angulation, deformities, swelling, bleeding, bony protrusions, obvious fractures or joint luxations, range of motion, atrophy, knuckling, and crepitus were examined. Skin and hair coat was examined for alopecia, masses, parasites, dryness, excessive oil, and matting. The palpate pelvic region was palpated for conformation and symmetry. The vertebral column was palpated to assess for deviations and pain. Peripheral lymph nodes (PLN) were palpated: submandibular, prescapular, axillary, inguinal, and popliteal. Thorax was observed and palpated for conformation, symmetry, and masses. In cardiac auscultation (CV) and respiratory auscultation (RESP), we first listened for noisy

Table 1: Clinical examination findings

Clinical examinations	Value	References	Index
Hydration status	Moderate(w~8%)	Euhydrated (standard), Mild (w~5%), Minimal loss of skin turgor, semidry mucous membranes, normal eye. Moderate(w~8%) Moderate loss of skin turgor, dry mucous membranes, weak rapid pulses, enophthalmos. Severe (.>10%) Considerable loss of skin turgor, severe enophthalmos, tachycardia, extremely dry mucous membranes, weak/thread pulses, hypotension, altered level of consciousness	%
Vital signs			
Body weight	115.3 kg	110-130	kg
Temperature	40.6	37.8-39.4	C°
Heart/pulse rate	109	56 to 97	bpm
Respiratory rate	10.3	8.4 ± 3.6	bpm
Perfusion indices(CRT)	2.8	≤ 2 seconds	SE

breathing at the mouth and nares without a stethoscope. We auscultated at least four chest areas, including right and left ventral and right and left dorsal lung fields. We heard 'Rales/crackles.' then we examined the Abdomen (ABD) and inspected for distention, deformity, displacement, symmetry, and bruising and auscultated the abdomen to detect intestinal hypermotility or hypomotility. Then we Palpated and visually assessed mammary glands for tumours, cysts, swelling, heat, or discharge and Inspected the vulva for size, inflammation, discharge (blood, pus), polyps, tumours, or structural defects. In the final stage, we determined the appropriate RAC Score for the animal. The area between the fourth and sixth intercostal spaces on both sides of the thorax was Palpated for the point of maximum intensity (PMI) of the heartbeat and any cardiac thrills. Heart rate (HR) and rhythm were evaluated, and Sinus arrhythmia and muffled heart sounds were heard. Examination of the body showed signs of superficial scratches on the left arm and palm and swelling and inflammation in the neck. Therefore, the neck area was immediately inspected by Time-of-Flight (TOF) MRA, imaging, and radiography (Figures 1 and 2).

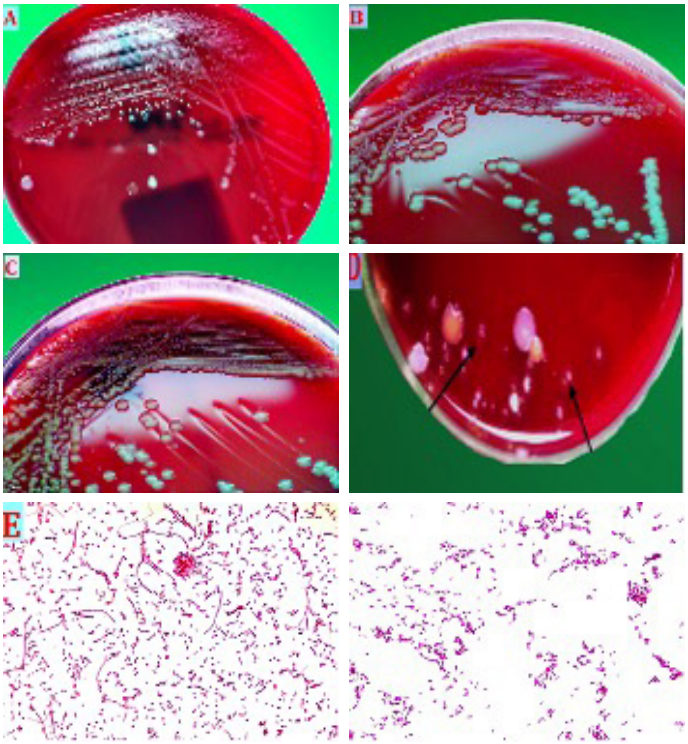

Figure 1: Morphological characterization of *Bergeyella (Weeksella) zoohelcum*. A, B: Bacterial colonies after culturing for 48 h on CBA (Columbia blood agar) (NCM0031A, Neogen ind., 620 Lesher Place Lansing, MI 48912 USA) C, D: colonies after culturing for 120 h on CBA. E: *Bergeyella (Weeksella) zoohelcum* staining properties. (gram staining, scale bar = 15 µm).F: *Bergeyella (Weeksella) zoohelcum* (acid stains quickly scale bar = 15 µm)

Sampling for clinical examination

At the same time of anaesthesia, chest and cervical X-rays, blood samples, and blood cultures were taken for clinical and microbiological evaluation (Figure 3). Empiric antimicrobial therapy was done using intravenous injection of Amoxirum Forte®300 mg (amoxicillin-sulbactam combination injectable antibiotic. Virbac, Pharmaceutical company, Carros, France), METACAM® (meloxicam, Boehringer Ingelheim. The pharmaceutical company, Ingelheim am Rhein, Germany)at the dosage (22 mg/kg), 0.2 mg/kg SC once then 0.1 mg/kg PO SID × 2d), and fluid therapy with Isotonic crystalloid solutions (lactated Ringer's solution plus dophalyte, Zoetis Pharmaceutical company, Parsippany-Troy Hills, New Jersey, United States)

Establishment of treatment protocol

After determining the results of haematology, microbiology, Time-of-Flight (TOF) MRA, imaging, and radiography and according to the antibiogram results, the initial treatment

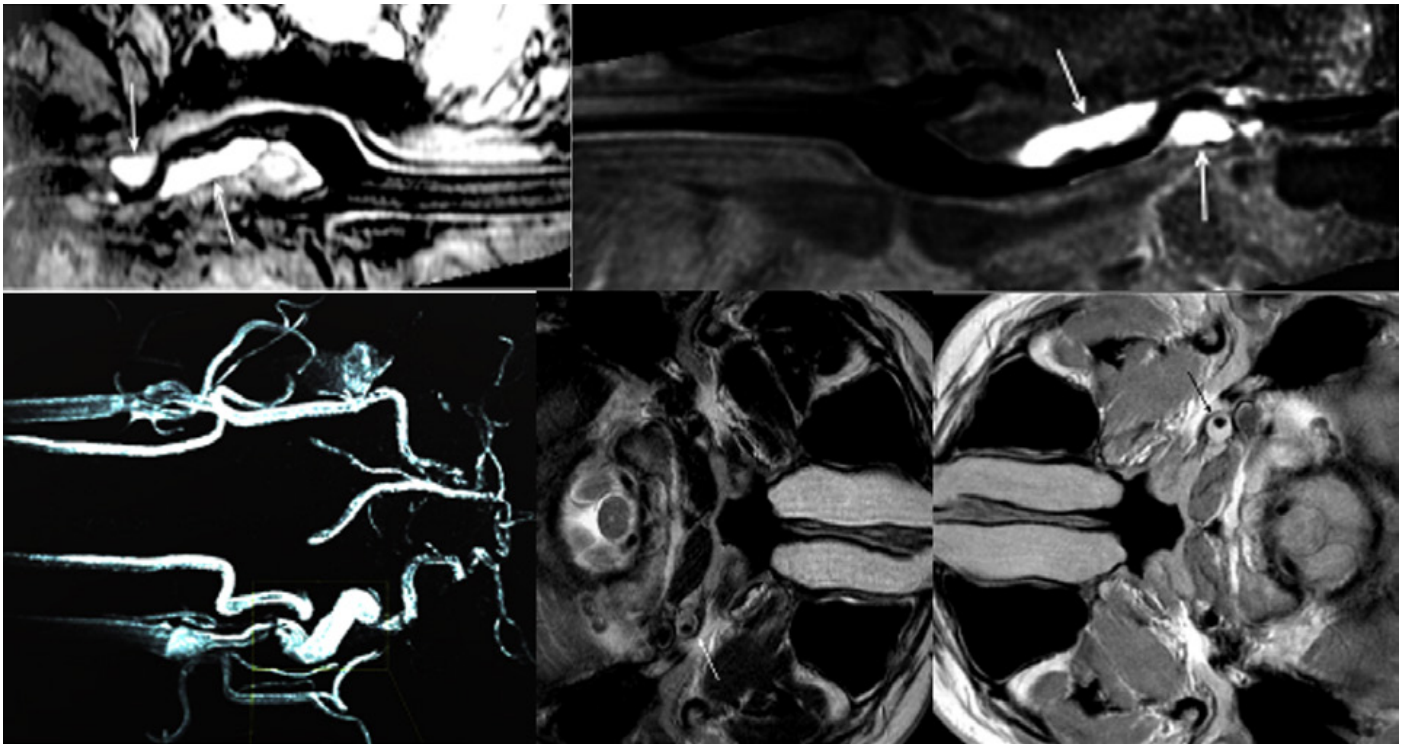

Figure 2: Unenhanced 2D TOF MRA of the craniocervical arteries: intra-cranial arteries 2D TOF (time-of-flight) demonstrates a patent left vertebral artery (major artery in the neck. It branches from the subclavian artery) (D). The MIP subvolume of the posterior circulation (consists of the two vertebral arteries, basilar artery, two posterior cerebral arteries, and their branches) (E) shows an irregular, stenotic mid-left vertebral artery initially felt to indicate a dissection. Axial reformatted source images show multiple small ring-shaped areas of signal severity corresponding to small cervical vessels (arrow, A). The interposition pattern created by these target patterns distorts the left vertebral artery that originates from the subclavian arteries, resulting in ill-defined or spiculated borders when compared with the right vertebral artery (Hitachi MRP 7000 MRI, Viable Med Services28470 Westinghouse Pl. Valencia, CA 91355)

process was confirmed. During the following days, the treatment was continued, and in order to facilitate the animal's breathing, after Wound Debridement, the tiger was intubated despite the concern about the exacerbated injury. Also, we use KENGREAL® (cangrelor) 30 mcg/kg IV bolus immediately followed by a four mcg/kg/min IV infusion to prevent blood coagulation. (The Medicines Company, Biotech company, Parsippany-Troy Hills, New Jersey, United States) for one week, then change to a dual therapy using Plavix® (clopidogrel) (18.75 mg PO q24h) (Bristol-Myers Squibb - Sanofi Pharmaceuticals, and XARELTO® (rivaroxaban) (2.5 mg PO q24h) (Janssen Pharmaceuticals, Inc., Beerse, Belgium) But Due to the severity of the injuries inflicted on the neck of the female tiger, the treatment was inconclusive. Twenty-eight days after causing the injury, the tiger died. After the death, a necropsy was performed, and all body organs were carefully inspected.

Genus identification of the isolate and genus-specific primers for the PCR identification

After receiving the initial microbiology results, to confirm the genus identification results of the isolate, PCR amplification of the 16S rRNA gene fragment by use of the primer set (forward primer 5'-AGA GTT TGA TCC TGG CTC AG-3' and reverse primer 5'-AAG GAG GTG ATC CAG CC-3') (Cat. Number: UN-PR001-005, Synbio Technologies,4250 US-1 Suite 3, Monmouth Junction, NJ 08852, United States) sequenced. Ribosomal RNA sequences were checked for the best match returned with the 16S-ribosomal rRNA gene database at NCBI.

Histopathology and immunohistochemistry techniques

In this study, depending on the conditions and needs, various diagnostic and immunohistochemical techniques were used as follows:

Verhoeff-Van Gieson (VVG) Staining Protocol

We used NovaUltra H&E Stain Kit (IHC-IW-3100) (Hölzel Diagnostika Handels GmbH, Germany) for this staining. First, we Deparaffinized and hydrated slides to distilled water. Then we Stained in Verhoeff's solution for 1 hour. The tissue should be completely black. After this step, we rinsed in tap water with 2-3 changes. Then we differentiated in 2% ferric chloride for 1-2 minutes. Moreover, Stop differentiation with several changes of tap water and check microscopically for black elastic fibre staining and grey background. It is better to slightly under-differentiate the tissue since the subsequent Van Gieson's counterstain can extract the elastic stain somewhat.

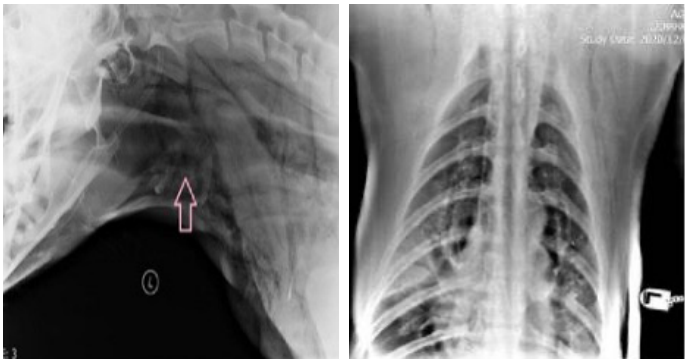

Figure 3: Neck and thorax radiography: Neck and thorax radiographic regions show significant amounts of gas density seen subcutaneously in the cervical region, which is extended up to the lateral aspect of the left thoracic wall—visibility of great vessels in the cranial mediastinum. The alveolar pattern, especially in the ventral aspects of lung lobes in the thoracic cavity, is noticeable. Lobar signs are also seen in the left middle lung lobe due to lobar consolidation. The presence of strip signs in the cervical region is probably secondary to gas densities within the oesophagus due to the anaesthesia process and respiratory distress. The diaphragm and rib cage are intact. No sign of pneumothorax is seen in the current radiographic examination (Veterinary X-ray system Maxivet 300 HF FF, COMES ELECTRO SRL, Via dell' Industria, 54 - 21044 Cavaria con Premezzo (VA) Italy).

Then we Washed slides in tap water. And then, we Treated it with 5% sodium thiosulfate for 1 minute and Discarded the solution. After this step, we washed in running tap water for 5 minutes. Moreover, we Counterstain in Van Gieson's solution for 3-5 minutes. Then we dehydrated quickly through 95% alcohol, two changes of 100% alcohol. Then we clear in 2 changes of xylene for 3 minutes each. And finally Coverslip with a resinous mounting medium

Immunohistochemistry Iba1 Antibody Staining Protocol

Iba1 (Allograft inflammatory factor 1 or ionized calcium-binding adapter molecule 1) is a 17-kDa EF-hand protein specifically expressed in macrophages and microglia and is upregulated during the activation of these cells.

Antigen retrieval (AR) method

Formic acid treatment: Free-floating tissue sections were incubated in 98% formic acid (EMD) inside closed 5 mL Eppendorf plastic tubes for 5 min at room temperature In a chemical fume hood, followed by removal for chemical waste disposal. The sections were immediately rinsed with room temperature ultrapure Type I water for 5 min, followed by two additional 5 min incubations in ultrapure Type I water.

Immunostaining

After antigen retrieval methods, free-floating Brain tissue sections were transferred to plastic mesh 70 µm cell strainers inserts (352350, BD Falcon, Franklin Lakes, New Jersey 07417, USA) and placed into six-well Cellstar plastic cell culture dishes (657-160, Greiner Bio-One North America, 4238 Capital Dr #7681, Monroe, NC 28110, United States) without lids for immunostaining. For immunostaining, slide-mounted sections were laid flat into a Prohisto slide staining container (Staining chamber StainTray™ Black lid, Sigma-Aldrich, St. Louis, Missouri, United States). All rinses and incubations were performed by placing the six-well plates of free-floating tissue onto a 55S Single Platform Shaker set at ten rocking motions per minute (Reliable Scientific, Inc., 1160 Thousand, Misty Oaks Ln, Hernando, MS 38632, United States). All free-floating or slide-mounted tissue sections were briefly washed in PBS for 5 min and then incubated with 0.3% H2O2 in PBS for 5 min at room temperature to inhibit endogenous peroxidase activity. A quick wash with PBS followed that for 5 min. For anti-Iba1 staining, free-floating tissue sections or slide-mounted tissue sections were blocked in PBS solution (PBS with 0.5% bovine serum albumin, BSA, 5% goat serum, and 0.1% Triton X-100) for one h, and then incubated in primary antibody in PBS solution (1:1000 anti-Iba1, rabbit polyclonal, 019-19741, Wako Pure Chemical Industries, Ltd, Wako Chemicals USA, Inc., Shibayagi Co., Ltd.,) overnight at four °C. After primary antibody incubation, the free-floating tissue or slide-mounted tissue sections were rinsed four times, 10 min each (with the PBS solution), then incubated with biotinylated anti-rabbit secondary antibody (1:2000, Vector Laboratories, Newark, California) for two h at room temperature. The secondary antibody was removed, and the free-floating tissue or slide-mounted tissue sections were rinsed four times with PBS solution and then incubated with PBS-Avidin-Biotin solution (2 µL each of solutions A and B per mL of PBS, Vectastain ABC kit, Vector Laboratories, Newark, California) for two h at room temperature. The free-floating tissue or slide-mounted tissue sections were rinsed four times with PBS only, then incubated for 5 min with a Vector VIP chromogen solution according to the manufacturer's instructions (Vector VIP peroxidase substrate kit, Violet SK-4600, Vector Laboratories, Newark, California) to develop the immunostains.

Immunohistochemical staining for glial fibrillary acidic protein (GFAP)

Glial fibrillary acidic protein (GFAP) is an astrocytic biomarker for the diagnosis, monitoring, and outcome prediction of acute brain ischemic stroke. GFAP is the major protein component of intermediate glial filaments, which increases within astrocytes in response to acute brain ischemic stroke. The slides were stained with a polyclonal rabbit GFAP antibody (GFAP Antibody (PA1-9565), Thermo Fisher Scientific, Waltham, Massachusetts, United States), dilution 1:4000, performed with a fully automated immunostainer (Oncore™ ProAutomated Slide Stainer from BIOCARE MEDICAL, 60 Berry Dr Pacheco, California 94553, United States) using DAB as the standard chromogen. After staining and preparing the slides under the microscope, characteristics such as nucleus morphology, nucleolus location, and cell borders were used to differentiate neurons from non-neuronal cells as established morphological criteria.

After the neurons' immunopositivity for GFAP was noted, the slides were stained analogously per immunolabelling and counterstained with hematoxylin.

Luxol Fast Blue–PAS staining

This method stains myelinated axons on formalin-fixed, paraffin-embedded brain tissue sections.

The myelin, including phospholipids, will be stained blue to green, and the neurons will be stained violet. To perform this procedure, we first Deparaffinize and hydrate sections to 95% ethyl alcohol, then we leave the sections in luxury fast blue solution overnight in a 58 C oven. Then we Rinse off excess stain with 95% ethyl alcohol and Rinse in distilled water. After this step, we differentiate the slides in the lithium carbonate solution for 45 seconds, then continue differentiation in the 70% ethyl alcohol for 40 seconds and rinse in distilled water. Then we Check the slides microscopically to see if the grey matter is straightforward and the white matter is sharply defined. Then we place the slides in distilled water and counterstain in the cresyl violet solution for 40-50 seconds. Then we rinse in distilled water and differentiate the slides in 95% ethyl alcohol for 4 minutes and 100% alcohol for 2x5 min, and xylene for 2x5 min. Finally, we mount with a resinous medium.

Results

Microbiology and blood biochemistry results

Bacteriological examination showed that catalase, urea, oxidase, and indol tests were positive, and Deoxyribonuclease (DNase) and Pyrrolidonyl Arylamidase (PYR) tests were negative. Initially, the isolate was misidentified as Bergeyella porcorum ATCC type strain 1350-03 by The MicroSEQ Rapid Microbial Identification System with Applied Biosystems™ components—only 83.2% identity (Thermo Fisher Scientific, Waltham, Massachusetts, United States). However, after the PCR, the results indicated the *Bergeyella zoohelcum*, ATCC 43767 type strain, with 97.9% identity. In contrast, the next best match was the Riemerella columbipharyngis, ATCC 8151 strain, with only 90.8% identity. Although, According to the principle of the extended phenotype, the identity algorithm of The Clinical & Laboratory Standards Institute guideline Anti-PD-1 Mouse Monoclonal Antibody (APC) (10377-MM18-A), about glucose non-fermenting Gram-negative bacilli, the 98.9% identity of this *Bergeyella zoohelcum* strain was lower than the requirement of ≥99.0% identity (With >0.7% allopatric speciation); In general, both based on the biological data obtained and based on the results of gene bank similarity measurement for 16S rRNA gene sequencing data supported the identification of *B. zoohelcum*. Weak growth of *Bergeyella zoohelcum*, ATCC 43767 was observed on CBA (Columbia blood agar) (NCM0031A, Neogen and., 620 Lesher Place Lansing, MI 48912 USA) after 48 h of incubation at 37°C. The stained strain was gram-negative, oxidase, and indole-positive (Figure 1).

This study is the first officially recorded finding of this bacterium in this animal species. Aerobic cultures from the wound surface tissue grew Pasteurella multocida, *Bergeyella* (*Weeksella*) *zoohelcum*, and two other gram-negative bacilli. These were subsequently identified as most as CDC group EF-4b and common species by the Tehran University Laboratory for Bacteriology, Veterinary Laboratory Centre for Disease Control in Tehran, Iran, based on cellular fatty acid composition data and biochemical reactions. Also, blood biochemistry findings are given in Table 2.

Results of the diagnostic imaging

According to the radiological observations, the Initial diagnosis was "open wound and subcutaneous emphysema" that was probably associated with an infective process in the cervical region and *pneumomediastinum*. Moreover, because we could not rule out the possibility of tracheal perforation in plain radiographs, the neck area was inspected by Time-of-Flight (TOF) MRA, imaging, and radiography (Figures 2 and 3).

Necropsy findings

The applied necropsy techniques enabled us to demonstrate the compound mechanism that inflicted them, combining penetration of tissues by the canines, crushing, and distension. Analyzing these wounds might reveal the motivation behind the injuries and the wild cat species involved in the attack. A tiger injury is sometimes compared with a scalpel injury, as multiple penetrating, scalpel-like ulcers characterize the patterned injuries due to a tiger bite. As a result, special attention is paid to determining the cause of death from bites by animal teeth under unknown trauma circumstances.

Gross Necropsy Findings in the Head and Nec

Traces of claws and tiger canine teeth indicate that the victim female tiger of the attack was knocked down from the ventral surface, along with profound and multifocal fatal wounds to the cervical region. The neck area was crushed due to the pressure caused by the force of the fangs (transfixing ulcer) and was violently expanded. In this area and on the skin, there were six deep and blunt wounds and traces of fangs. The cervical area indicated massive damage, including tearing the oesophagus, trachea, and muscles, and inflammation of vertebrae C1 and C4 with internal channels resulting directly from penetration by the tiger's fangs. The expansion of the muscles happened because of the vigorous movements of the male tiger's head while trying to suffocate the female tiger, which led to the rupture of vertebral arteries.

Table 2: Haematological and biochemical results. (41)

Parameters	Result	Reference	Parameters	Result	Reference
Glucose (mg/dL)	127	88-183	AST (IU/L)	370	14.4–84.0
Triglyceride (mg/dL)	110	25-165	ALT (IU/L)	46	21.2–109.0
Cholesterol (mg/dL)	176	77 - 253	ALP (IU/L)	13	13 - 71
Albumin (g/dL)	3.83	2.1–4.6	GGT (IU/L)	3.5	1-10
Total protein (g/dL)	6.5	3.7–8.7	CK (IU/L)	5903	69 - 893
Globulin (g/dL)	5.3	2.8 - 4.8	Amylase (IU/L)	585	100-1200
A/G	0.7	0.8–1.00	Lipase (IU/L)	11	10-450
Urea (mg/dL)	187.3	5.50–27.70	Total bilirubin (mg/dL)	4.9	0.4–3.2
BUN (mg/dL)	87.52	6.5–48.2	Direct bilirubin (mg/dL)	3.69	0.09-1.9
Creatinine (mg/dL)	7.2	1.6–4.6	Calcium (mg/dL)	13.1	7.53-14.7
Phosphorus (mg/dL)	28.6	2.2 - 5.5	Uric acid (mg/dL)	1.2	0.32-1.8
HCT (%)	57.2	34 - 48*	PLT (%)	0.09	0.07-1
RBC ($\times 10^6$/µL)	7.51	7.5 - 11.7	MPV (fL)	11.4	10-12
HGB (g/dL)	13.5	11.5 - 15.9	NCC^ ($\times 10^3$/µL)	9.1	8-10
MCV (fL)	52.3	36 - 46	Segs ($\times 10^3$/µL)	4.43	4-5
MCH (pg)	19	12.5 - 16.4	Bands ($\times 10^3$/µL)	3.91	0.0 - 4.0
MCHC (g/dL)	36.3	32.2 - 36.8*	Lymphs ($\times 10^3$/µL)	0.27	1.05 - 8
PLT ($\times 10^3$/µL)	168	169 - 480	Monos ($\times 10^3$/µL)	0.18	0.1 - 0.3
RDW-CV (%)	14.8	12-16	Eos ($\times 10^3$/µL)	0	0.2 - 1.1
RDW-SD (fL)	31.4	30-34	Baso ($\times 10^3$/µL)	0	0-4
D-dimer	1673	< 250 ng/ml	blood FDP	35	10 (µg/ml)

A/G = albumin/globulin ratio, ALP= Alkaline phosphatase, ALT= Alanine transaminase, AST= Aspartate transaminase, Bands= Band Cells, Bso= Basophils, BUN= Blood Urea Nitrogen, CGT = Gamma-Glutamyltransferase, CK = Creatine Kinase, Eos = Eosinophils, Fl = femtoliter, g/dL= Grams Per Deciliter, HCT= Hematocrit, HGB= Hemoglobin, IU/L= International Units Per Liter, Lymphs = Lymphocytes, MCH = Mean corpuscular haemoglobin, MCHC =Mean Corpuscular Hemoglobin Concentration MCV = Mean Corpuscular Volume, mg/dL= Milligrams per decilitre, Monos= Monocytes, MPV=Mean platelet volume, NCC= Nucleated cell counts, pg = pictogram, PLT = platelets, RBC = Red Blood Cell, RDW-SD = Red Cell Distribution Width Standard deviation, RDW-CV= Red Cell Distribution Width Coefficient of variation, Segs= Neutrophils, µL=microliter FDP= Fibrin Degradation Products. D-dimer(a fibrin degradation product, a small protein fragment in the blood after a blood clot is degraded by fibrinolysis).

Moreover, an intramural rupture of the carotid arteries during the tiger's battle has never been described. Therefore, a detailed necropsy was performed to evaluate the amount of bone damage and the injury to the spinal canal. The applied necropsy techniques enabled us to demonstrate the compound mechanism that inflicted them, combining penetration of tissues by the canines, crushing, and distension. Analyzing these wounds might reveal the motivation behind the injuries and the wild cat species involved in the attack.

A tiger injury is sometimes compared with a scalpel injury, as multiple penetrating, scalpel-like ulcers characterize the patterned injuries due to a tiger bite. As a result, special attention is paid to determining the cause of death from bites by animal teeth under unknown trauma circumstances.

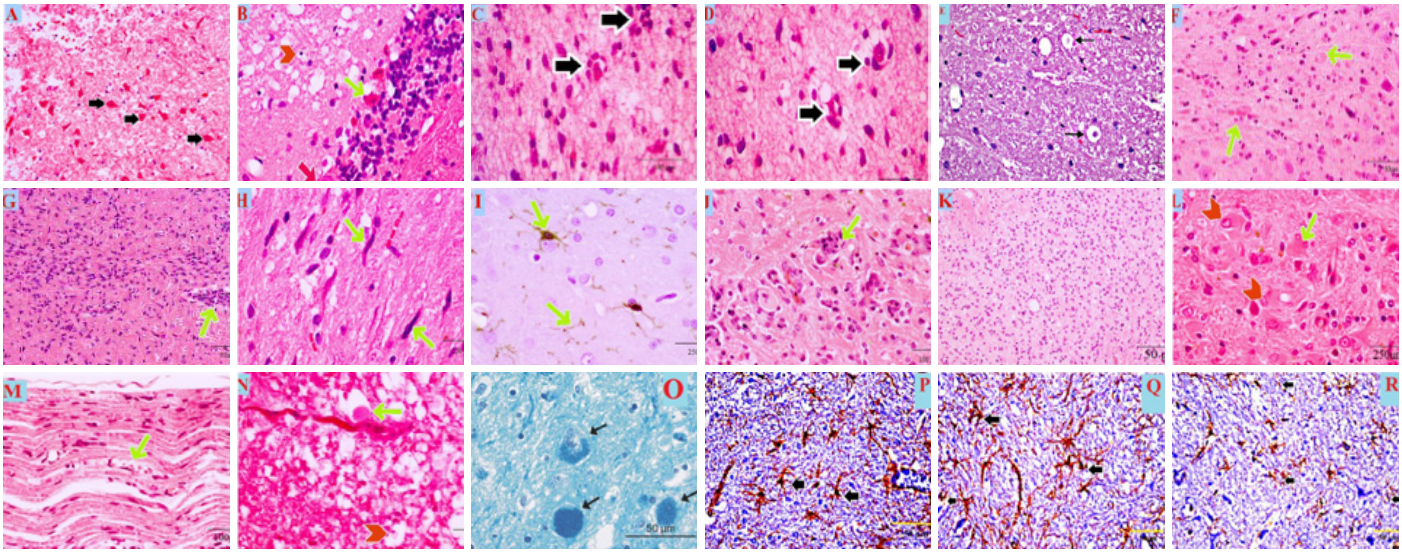

Figure 4: Cerebral Parenchyma Histopathological changes in transient ischemic attack A: red neurons (Yellow Arrows). (Hematoxylin and Eosin Staining, Scale Bar=μm). B: red neurons (Yellow Arrows), normal neuron (Pink Arrow), and pyknotic nucleus along with vacuolation of the neuropil(Red Head Arrow).C&D: perineuronal satellitosis, increase in the number of cells encircling a neuron(Yellow Arrows). (B, C, D: Hematoxylin and Eosin Staining, Scale Bar=100μm). E: Swollen and degenerated axons without myelin sheath are seen. (Yellow Arrows),F: A bubble-like biological feature(Axonal spheroid) is seen in the degenerated axon(Yellow Arrows). G: Various irregular, elongated nuclei of microglial cells formed as a Microgliosis near the inflammatory mononuclear perivascular cuffing (Yellow Arrow). (E, F, G: Hematoxylin and Eosin Staining, Scale Bar=50μm). H: irregular nuclear of microglial cells (Yellow Arrows). (H: Hematoxylin and Eosin Staining, Scale Bar=250μm). I: Immunohistochemical staining using Iba-1 antibody to visualize microglial cells(Yellow Arrows). J: Reactive gliosis and Hyperplastic capillaries (Yellow Arrow). (I,J:Iba1 Antibody Staining, Scale Bar: I=250μm,J=100 μm) K: Increase in nucleated cells Consisting of reactive astrocytes, macrophages, and mixed gliotic response. L: Reactive gemistocytes astrocytosis. Eccentric nucleus, prominent eosinophilic cytoplasm of reactive astrocytes (Red Head Arrows), and the less frequent micro-binucleate (Yellow Arrow). M: Wallerian degeneration(axonal fragmentation) (Axonal spheroid). N: A large swollen axon (pre-degenerative changes) and a degenerate macrophage in the necrotic axon space. (K, L, M, N: Hematoxylin and Eosin Staining, Scale Bar: K=50μm, L= 250μm, M=100 μm, N= 250μm).O: cerebrum: Intracytoplasmic Luxol fast blue positive pigments are seen in the neurons. (Black Arrows)(Luxol fast blue staining, Scale Bar=50μm). P: Short cytoplasmic processes of the astrocytes(Black Arrows). Q: Brown cytoplasmic granules in the neuroplastic astrocytes(Black Arrows). R: Degenerating and dead Astrocytes are seen. (Black Arrows). (P, Q, R: glial fibrillary acidic protein (GFAP) Staining, Scale Bar=50μm).

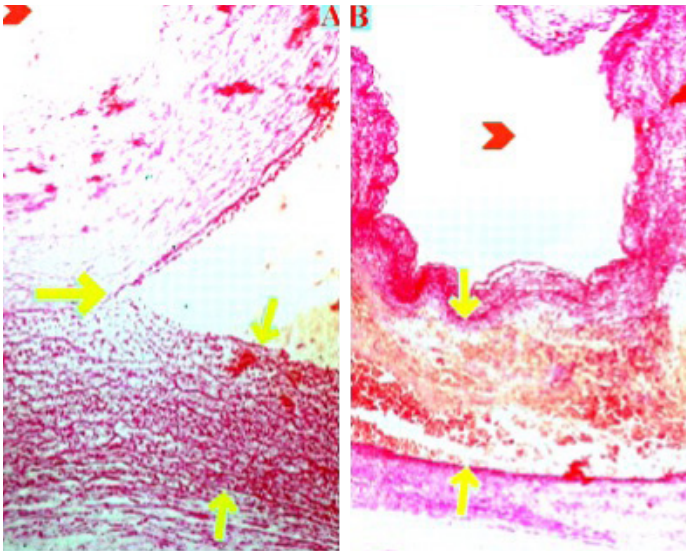

Figure 5: Intramural hematoma of the mid-left vertebral artery(major artery in the neck branches from the subclavian artery) (A) the arterial wall zipper-like separation, mucoid degeneration, and false lumen of the tunica media (Yellow arrows). (B) A cross-section of the dissected artery shows intermedial and subintimal hematoma (Yellow arrows). Red Head Arrow (lumen); Elastica van Gieson staining NovaUltra H&E Stain Kit (IHC-IW-3100)(Hölzel Diagnostika Handels GmbH, Germany), scale bar = 0.25 mm

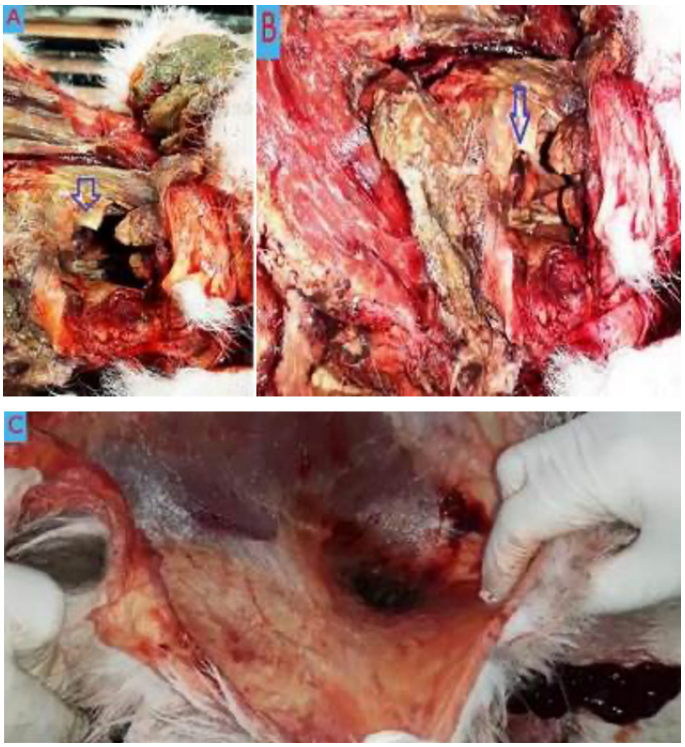

Figure 6: A and B: Complete rupture of the trachea. C: Skin blunt trauma

Brain

Red neurons appear in the earliest phase of infarction, consisting of increasing cytoplasm eosinophilia with the nucleus shrunken and basophilic. Then the cytoplasm becomes uniformly structureless, and the nucleus shows homogeneous degeneration. In the late stage, the neurons are disintegrated, resulting in eosinophilic debris dispersed throughout the neuropil and scattered eccentrically from the remainder of the dead neurons. Later, all these remains were phagocytized by foamy macrophages (ghost neurons). Finally, eosinophilic ischemic neurons spread and disseminated among the normal-looking neurons and were surrounded by an increased number of oligodendrocytes (steatosis). Around dying neurons, the microglial cells retract their processes and assume an amoeboid morphology, becoming activated (Figure 4).

Cervical Part

In the cervical region necropsy, complete rupture of the trachea was observed from two places (connection to the larynx) and 3 cm below it, as well as lateral and vertical rupture of the oesophagus with a length of 5 cm and rupture of the left subclavian artery, left vertebral artery, left common carotid artery. The rupture of these arteries led to extensive extravasation at the back of the throat and larynx (Figure 5).

Extensive adhesions and focal necrosis were also observed in the pectoralis area and on the *pectoantebrachialis*, *sternomastoid*, and *pectoantebrachialis* muscles that continued until the beginning of the *xiphihumeralis* area, which was filled with exudative and mucoproliferative secretions and a prominent inflammatory infiltrate into the subcutaneous space. Examination of the internal organs of the lungs revealed extensive pneumonia in both lungs, the development of interstitial bronchopneumonia and marbled of the lungs, and the effect of the ribs on the lungs due to pressure in the thoracic region. Lung tissue was full of foamy discharge due to weather and severe respiratory distress (Figure 6).

Pathological injuries, longitudinal tears, thinning, and loss of elastic fibres are well-defined using Verhoeff-Van Gieson elastic staining. This staining is a simple method that is used for visualizing elastic fibres.

Postmortem examination of the Thoracic Cavity

Trachea

Squamous metaplasia in the trachea epithelium with intense chronic inflammation visible in the submucosa, including cicatrization. The underlying cartilage indicated sequestration along with ossific metaplasia. By far, the most pathological changes included diffuse paracellular or hyperplastic fibrosis with intense hyperplastic scar formation or hyaline cicatrization found in the outer part of the perichondrium overlying adventitia. In the membranous portion, severe scar formation and hyperplastic fibrosis were predominant. Metaplastic pulmonary ossification was exclusively severe in the outer and lateral parts of the tracheal ring, particularly in the vicinity of the adventitia and outer perichondrium (a layer of dense irregular connective tissue). These changes were much more pronounced than the relatively minor changes observed in the mucosa and submucosa (Figure 7).

Lung

The pathophysiology of this injury was blunt chest trauma and pulmonary contusion, including pulmonary oedema, inflammation, enlarged basement membrane thickness,

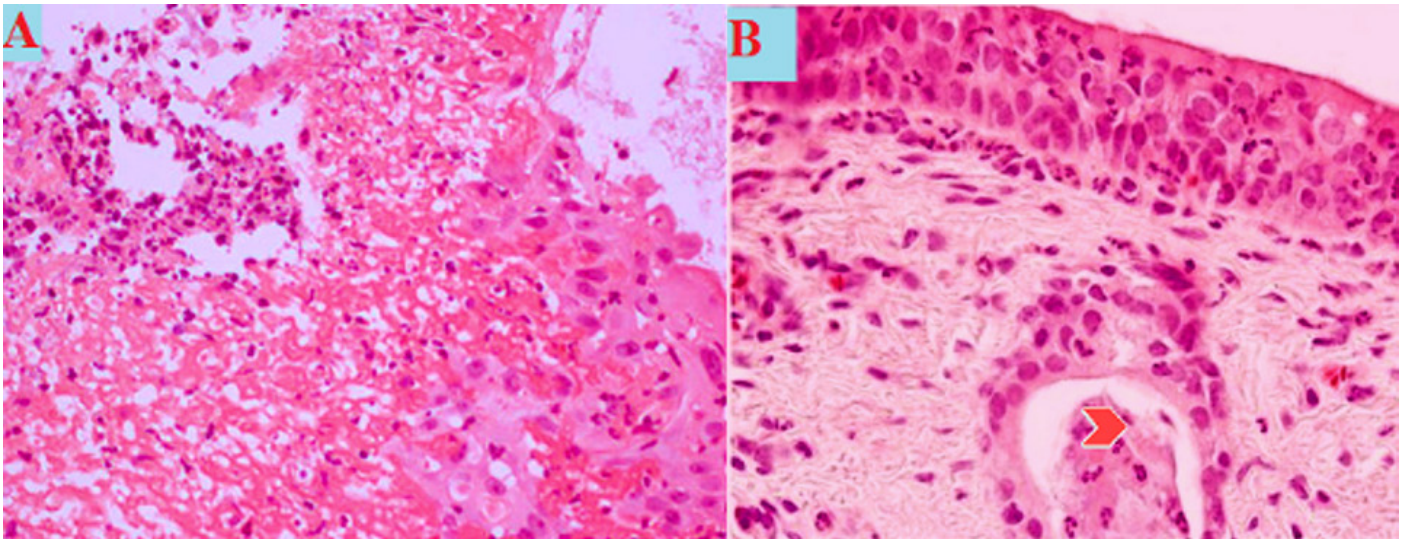

Figure 7: Occasional chronic inflammation along with squamous metaplasia A: Massive ulceration of the tracheal mucosa and abundant neutrophils admixed with pale extracellular eosinophilic material (oedema) within the submucosa and lamina propria (100×. H& E). B: A few lymphocytes are present within the lamina propria and submucosa and accumulation of cellular debris and neutrophils in the submucosal gland (Red Head Arrow), (H&E stain, 400×)

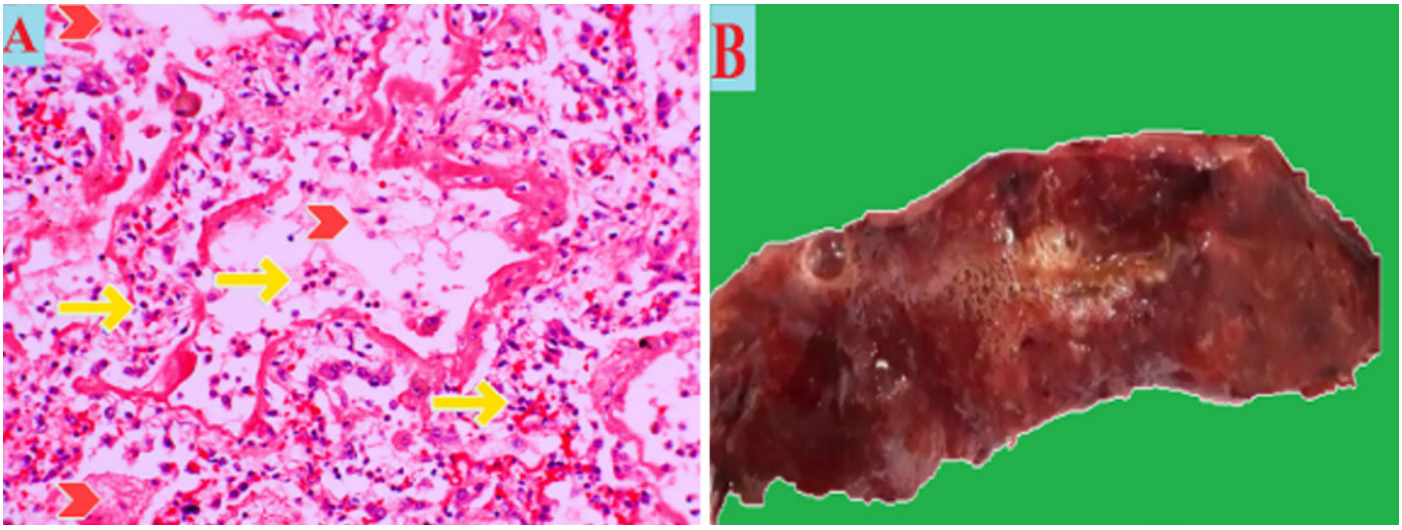

Figure 8: Diffuse alveolar damage. (A) The pulmonary alveolus is lined by hyaline membranes(Red Head Arrows). Immature fibroblasts and macrophages are present in different parts of the lung tissue, such as inside the alveoli and the interstitial space (Yellow Arrows). H&E stain, 100× (B): Aspiration Pneumonia due to the widespread inflow of fluid into the lungs, a substantial volume of fluid in the lung tissue that flows rapidly with low pressure. Putrefactive Disorganization and discolouration pneumonia caused ill-defined brownish-yellow (amber) areas of softening in the lung and necrotic slimy contents in the centres with malodor(stench)

increased diffuse alveolar damage, perfusion mismatching, cellular infiltration, increased intrapulmonary shunting, and a loss of compliance, injury to type 2 pneumocytes and endothelial cells. An area of oedema commonly surrounds the pulmonary contusion. Fluid accumulation in alveoli interferes with gas exchange and causes alveoli to be filled with proteins and collapse. Extensive pneumonia in both lungs and the development of interstitial bronchopneumonia and marbling of the lungs. Pulmonary contusion results in haemorrhage and exudate leakage into lung tissue, which becomes rigid and loses its average elasticity. The thin membrane between the alveolar sac and the capillaries is torn, and damage to the capillaries causes both blood and exudate to leak into the alveoli and the interstitial space of the lung parenchyma. Pulmonary contusion is characterized by micro-haemorrhages or microbleeds when the alveolar sac is traumatically separated from airway structures and capillaries (Figure 8).

Heart

Cardiac damage caused by ischemic coronary insufficiency may lead to fatal injuries and sometimes life-long heart problems. In most cases, mild and reversible damage, such as Takotsubo cardiomyopathy and neurogenic stress cardiomyopathy (Figure 9). A slight increase in cardiac enzymes characterizes takotsubo cardiomyopathy (Figure 10). Moreover, it is a sign of myocardial damage.

Other necropsy findings

The throat and larynx were completely erect and hemorrhagic. In the oesophagus, petechiae and foamy discharge, as well as symptoms of diverticulum and mega-oesophagus due to external pressure due to fluids, were evident. Gastric tissue contains small amounts of bloody secretions due to ingesting exudative fluids and blood from the bleeding throat and trachea. The liver has an average but inflamed consistency, and the kidneys have weak compensatory hypertrophy symptoms. Furthermore, in the cross-section, its radial lines were lost. Symptoms of interstitial nephritis and glomerulonephritis were seen. The spleen showed complete signs of lymphocyte depletion with atrophy.

Discussion

In human medicine, craniocervical artery dissection is one of the most common causes of stroke and severe brain damage in young and middle-aged adults (7). However, this injury has not been reported in animals, and this is the first recorded report of this condition in animals and wild carnivores.

This lesion initially started with the tear of the vessel's intima layer and was followed by the formation of an intramural hematoma (8). Most of these wastes occur spontaneously or after minor vessel trauma. Emergent assessment is required in these cases; recommended diagnostic tests are head and neck computerized tomography angiography with computerized brain tomography and head and neck magnetic resonance imaging (MRI) (9). In this study, we used the Time-of-Flight (TOF) MRA technique. The main advantage of the TOF-MRA technique is the direct visualization that uses the images in their original visible format of The Blood vessel walls and their interactions confirming the Intramural hematoma (IMH). Therefore, TOF- MRA is the method of choice for preliminary diagnosis and follow-up of craniocervical artery dissection. One of the most important complications of this study was determining the exact cause of TIA and stroke. Several factors have been introduced as triggers for stroke. Factors such as a family

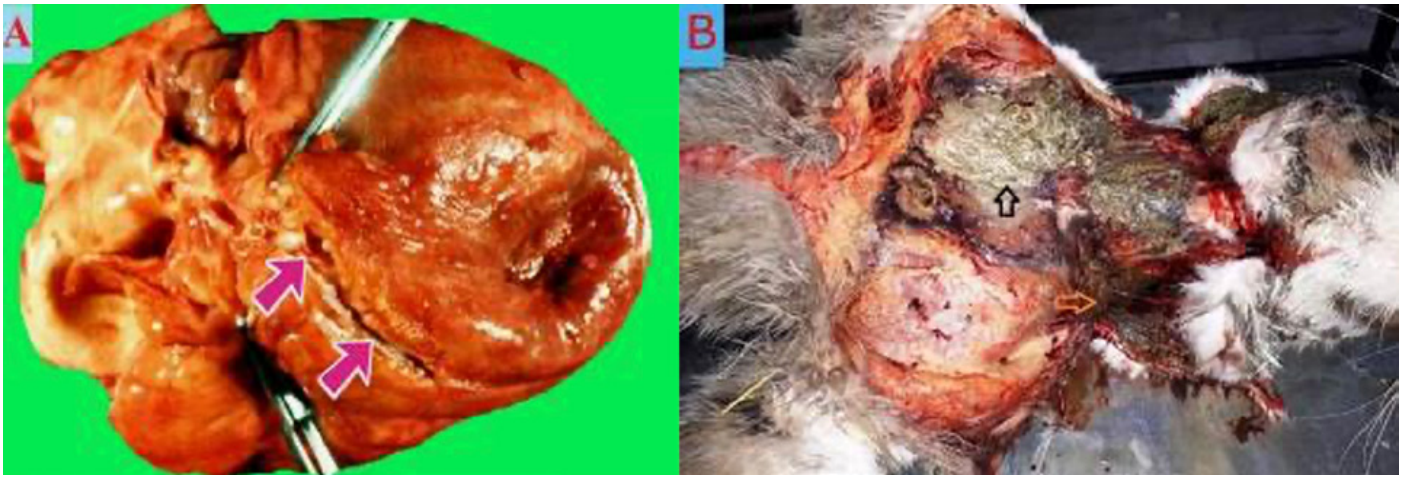

Figure 9: The myocardium was hypertrophic and flaccid. A: On cardiac examination, the myocardium was hypertrophic and flaccid. Also, postmortem thrombotic foci in cardiac septa and rough surfaces and ruffles on the Epicard layer indicate severe cardiac overload and output. B: Extensive adhesions. Additionally, focal necrosis was observed in the pectoralis area and on the pectoantebrachialis, sternomastoid, and pectoantebrachialis muscles that continued until the beginning of the xiphihumeralis area, which was filled with exudative and mucoproliferative secretions and a significant inflammatory infiltrate into the subcutaneous space

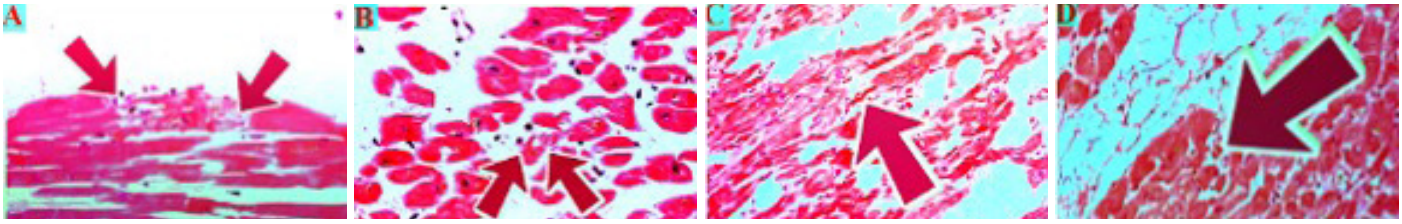

Figure 10: Tako-tsubo(ampulla) cardiomyopathy. A: Myocardial damage in the epicardium (outer layer). Apical posterior, external layer. H&E stain, x 400. B: Injured cardiac myocytes are removed by infiltrated macrophages and left ventricular apical, middle layer—Hematoxylin and eosin (H&E) stain, x 400

history of stroke or TIA, higher risk of TIA in males than females, high blood pressure, dyslipidemia, diabetes mellitus, Genetics, race, and imbalance in lipid profile, are other risk factors of TIA (10). However, in general, the predictive indices of cerebrovascular ischemia are still incomplete, which suggests that there may be risk factors that are not yet commonly recognized. Infections that occur acutely and suddenly in the body may be a risk factor for cerebrovascular ischemia, which has been underestimated. Bacterial organisms are the main cause of Brain stroke, among other infectious agents. Until the antibiotic era, rheumatic heart disease was a predisposing risk factor for infective endocarditis. (11). A positive correlation has been observed between the mortality rate of cardiovascular diseases and the epidemics of respiratory infections (12). In these cases, attention should be paid to important biochemical tests such as CRP with high sensitivity, number of leukocytes, blood sugar, and lipid profile. For example, the number of leukocytes is related to myocardial infarction and ischemic stroke risk. There is also clinical evidence of infections such as gastroenteritis, Respiratory tract infections (RTIs), and Urinary tract infection (UTI)., which are biochemically caused by leukocytosis and elevated levels of high-sensitivity C-reactive protein. Hence, these tests appear to be recognized early diagnostic tools with predictive value. They are good. Moreover, by paying close attention to them, early treatment of febrile illness and introducing or adjusting the dose of antiplatelet agents and antibiotics. can be determined to reduce the actual incidence of stroke. Considering the diagnosis of *Bergeyella zoohelcum* infection in this study, the existence of this infection can be considered an important risk factor. This case adds to the complexity of the final diagnosis of the chain of events leading to death in this study. The correlation between globulin and serum albumin with the Dissection of the Craniocervical Artery has been emphasized. Albumin and globulin are the most important components of feline blood serum proteins and play a major role in the body's systemic inflammatory processes. The data relating to serum albumin shows a valid indicator for evaluating the nutritional status as well as the status and degree of inflammation in the Craniocervical Artery Dissection. Also, an increase in serum globulin indicates the inflammatory response of the body and a response to the accumulation of various types of pro-inflammatory cytokines. On the other hand, hypoalbuminemia is associated with impaired survival rates in cases of Craniocervical Artery Dissection. Low globulin levels are a sign of liver and kidney insufficiency or malnutrition. Also, during kidney disorders such as nephrotic syndrome, this problem occurs due to the loss of proteins through renal filtration. On the other hand, An elevated globulin level (5.3) is independently associated with extravasation in intra-arterial thrombolysis and Vascular injuries such as rupture and inflammation. As it is clear from the results of

haematology studies, the ratio of albumin to globulin in this tiger is low and is around 0.72. A low albumin-to-globulin ratio has a high positive predictive value for Acute inflammatory processes. As a result, investigating these parameters justifies an acute inflammatory process following Craniocervical Artery Dissection. There are still uncertainties about the changes in these proteins and how they affect the occurrence or exacerbation of craniocervical pathological effects and Further research is needed in this field. As proven in previous studies, the CRP, blood urea nitrogen (BUN), and creatinine levels would be markedly elevated in craniocervical artery dissection and infarction of the Brain supplying arteries. It has also been proven that High blood urea nitrogen (BUN) is associated with an elevated mortality risk in various diseases, such as heart failure, pneumonia, and Dissection of different arteries. In this study, the amount of blood urea nitrogen (87.52), creatinine (7.2), and urea (187.3) were elevated, which confirms the occurrence of craniocervical artery dissection and the importance of these parameters in predicting the occurrence and evaluation of craniocervical artery dissection.Recent clinical studies have revealed that Craniocervical Artery Dissection is mediated by inflammation in the tunica adventitia and media of the vertebral artery, leading to degradation of the extracellular matrix, including elastin, collagen, enzymes, glycoproteins and hydroxyapatite and tearing in the medial tunica layer (13). According to histopathological analyses, macrophages and lymphocytes are recruited to the tunica media, and matrix metalloproteinase is involved in the degradation of elastin, collagen, non-collagen, and proteoglycan (14). Serum inflammatory markers, including CRP, serum amyloid A, cytokines, alpha-1-acid glycoprotein, plasma viscosity, ceruloplasmin, hepcidin, and haptoglobin, are often elevated in these animals. Interestingly, one observational study showed that the serum CRP level re-elevation is a useful marker of Craniocervical Artery Dissection (15). The authors speculated that local thrombogenesis triggers inflammatory cytokines, including interleukin-1(IL-1), IL-6, IL-12, IL-18, TNF-α, IFNγ, and GM-CSF that are released from immune cells like helper T cells, macrophages, and certain other cell types that promote inflammation, leading to increased production of CRP (16). Recent clinical studies have revealed that Craniocervical Artery Dissection is often accompanied by high levels of blood Fibrin Degradation Products (FDP) and D-dimer, indicating the presence of Basilar artery thrombosis and Intra-Arterial Thrombolysis and aiding in reaching The Accurate Diagnosis (17). Clinical guidelines for Craniocervical Artery Dissection state that a D-dimer level <250 ng/mL exhibits negative predictive value (NPV) for Craniocervical Artery Dissection in Felines presenting with traumatic injuries of the neck and chest area. In contrast, a D-dimer level >1400ng/mL exhibits a positive predictive value (PPV) (18). Indeed, in the present case, the D-dimer level was greater than 1,600 ng/mL (16,700 ng/mL), compatible with the typical paraclinical findings of Craniocervical Artery Dissection. In this study, the measurement of D-dimer level had diagnostic value because this parameter was measured within 11 hours after Craniocervical Artery Dissection. The observed hyperphosphatemia (28.6) was due to acute renal failure. A high serum CK value (5903) indicated muscle damage due to acute muscle injury within conflict. which had resulted in widespread acute rhabdomyolysis. A high level of AST (370) indicated inefficiency and acute liver and heart tissue damage due to the injury caused by the conflict and the effect on other organs. A high level of Direct bilirubin (3.69) was a sign of liver insufficiency, and a high level of total bilirubin (4.9) was also a sign of liver failure and widespread destruction of red blood cells due to injury and haemorrhage. higher amount of hematocrit (57.2), MCV (52.3), and MCH (19) indicated Dehydration due to haemorrhage, Lung and heart insufficiency, and anaemia.

Of course, the initial findings of this study and the course of the disease were such that, at first, it was more likely to be an acute traumatic injury instead of a longer degenerative lesion. However, when the disease took a chronic course and lasted for twenty-eight days, the occurrence of a chronic degenerative lesion was confirmed. As mentioned in the related texts, the cause of ischemic stroke is usually due to the complete loss of blood supply to the brain tissue, shown in this case. Moreover, since transient ischemic attacks usually do not cause ischemic stroke, the possibility of other factors being involved in causing stroke in this valuable species is raised, which, as mentioned at the beginning of the discussion, is one of the powerful and essential factors of bacterial infection.

In the acute setting, Craniocervical artery dissection may lead to a transient ischemic attack, Subarachnoid Hemorrhage, local compressive symptoms such as cervical radiculopathies, and cranial neuropathies (19). Therefore, intravenous thrombolytic therapy and, in select cases, mechanical thrombectomy are the Acute treatment of ischemic stroke in Craniocervical artery dissection (20). however, Anticoagulation should typically be avoided in intracranial craniocervical artery dissection (21). However, in the case of extracranial craniocervical artery dissection, despite no reliable and documented consensus on the strategy to prevent stroke, expert opinion favours Anticoagulation or dual antiplatelet therapy for at least six months (22).In a similar case of a young chimpanzee in Tehran's Eram Zoo, the author completely cured this problem with antiplatelet therapy for eight months. Therefore, young carnivores need Anticoagulation and antiplatelet therapy (23,24). Therefore, few side effects have been reported considering that dual antithrombotic treatment with clopidogrel and rivaroxaban is generally well tolerated in cats (25). Moreover, dual therapy may effectively prevent thrombosis in a high-risk population of cats with heart disease (26). Therefore, in this study, we decided to use these two drugs, and until the last day, when the animal died, at least the side effects caused by these drugs or blood coagulation problems were not observed.

Recurrent ischemic dissections are never reported in wild captive animals, but in human medicine are rare and occur in the first few months after diagnosis (27). There is a knowledge gap regarding the type of antithrombotic regimen, stenting, and duration of antithrombotic therapy for stroke prevention in craniocervical artery dissection (28). Therefore, because Recurrent ischemic dissections may occur if the tiger survives, from the very beginning of the diagnosis and for the first week, it was decided to use KENGREAL®. That is a direct P2Y12 platelet receptor inhibitor that blocks ADP-induced platelet activation and aggregation. Cangrelor binds selectively and reversibly to the P2Y12 receptor, preventing further signalling and platelet activation. Generally, A well-designed trial including advanced imaging and genetic biomarkers is required to compare various antithrombotic approaches, and stenting in craniocervical artery dissection is required (29).

For the first time, this study depicted the histopathological features of this condition in animals, including a scarce and endangered animal (white tiger). Moreover, in this sense, it has presented exciting findings.

Examining the results of this study shows a significant overlap in the histopathological findings of this condition in humans. The findings of this study in some tissues, such as the Brain and heart, are exciting and thought-provoking. Following the sequence of these events at the cellular level provides much help for the correct understanding of the lesion process from the time of emergence to death.

Another interesting finding of this study was accidentally obtained during sampling of damaged tissues. Moreover, It had no specific relation to the main finding of this study, i.e., Craniocervical Arterial Dissection was Isolation of *Bergeyella zoohelcum*, which is an aerobic, Gram-negative bacterium isolated from mammals' upper respiratory tract (30). *B. zoohelcum* has been reported to cause septicemia, tenosynovitis, and abscess, which relates to carnivores' bites (31). *Bergeyella zoohelcum* is susceptible to beta-lactams. It includes fluoroquinolones, ceftazidime, ceftriaxone, and penicillin and is variable in susceptibility to clindamycin, meropenem, and trimethoprim-sulfamethoxazole (32). Multiple reports have been associated with the wound, interstitial pneumonia, tenosynovitis, meningoencephalitis, abscesses, and cellulitis of the limbs, and only five cases of *B. zoohelcum* bacteremia have been reported before (33). Sharma reported detecting *B. zoohelcum* in Oral mucosal secretions of therapy toy dogs in close contact with the Elderly residing in a Retirement home (34). B*ergeyella zoohelcum* isolates were recovered from the lungs and tonsils of five deer, an 8-year-old female grey fox who developed bacteremia, nausea, fever, and diarrhoea after ingestion of donkey's meat (35). the source of B. zoolhelcum in animal infection is contact or exposure to foxes, wolfs, leopards, or contaminated food. In zoos, older dogs or cats may develop invasive diseases with *B. zoolhelcum* (36). Therefore, no antibiotic choice is recommended for *B. zoohelcum* infections (37). However, animals can be treated with agents that have been demonstrated effective against strains isolated from other animals (38). Meropenem, amoxicillin-clavulanic acid, ampicillin-sulbactam, ceftazidime, and marbofloxacin have successfully treated animals (39). In wild animal medicine, Betamax long act and etomoxir are appropriate for treating bite-related infections. It is a reasonable choice for co-infection with other pathogens, including *Pasteurella multocida* and anaerobes (40). However, the use of extended-spectrum antimicrobials for treating *B. zoohelcum* infection in the era of rising antimicrobial resistance deserves careful consideration (35).

Conclusions

This study showed that Craniocervical Arterial Dissection through multiple injuries leads to Transient ischemic attack in the Brain. Also, in this study, the bacterium *Bergeyella zoohelcum* was isolated for the first time, which is the first report of the isolation of this bacterium in a tiger. Our experience in this study showed that Craniocervical Arterial Dissection could cause many pathological injuries in different organs, the results of which are included in this study, also based on our experience, a quick and accurate accident diagnosis prevent many subsequent unfortunate events and can provide the basis for appropriate and optimal treatment in connection with the Dissection of the craniocervical artery. In the meantime, whole-body trauma computed tomography with an adapted scanning protocol for the craniocervical vessels is a safe, fast, and feasible method for detecting vascular injuries. It allows prompt further treatment if necessary. CTA could be a part of a broad screening protocol for craniocervical vessels in the documented head and neck injuries and trauma mechanisms influencing the craniocervical region.

Acknowledgements

The authors thank the Eram Zoo, Tehran, Iran, for their collaboration and support during all experimental research procedures.

References

1. Shi C, Xu J, Roberts NJ, Liu D, Jiang G. Individual automatic detection and identification of big cats by combining different body parts. Integr Zool 2023; 18: 157–68.
2. Xu X, Dong GX, Hu XS, et al. The genetic basis of white tigers. Curr Biol 2013; 23: 1031–5.
3. Xu X, Luo SJ. How the white tiger lost its colour but kept its stripes. Sci China Life Sci 2014; 57: 1041–3.
4. Marsh SME, Hoffmann M, Burgess ND, et al. Prevalence of sustainable and unsustainable use of wild species inferred from the IUCN Red List of Threatened Species. Conserv Biol. 2022; 36: e13844. doi: 10.1111/cobi.13844.

5. Bachmann ME, Kulik L, Gatiso T, et al. Analysis of differences and commonalities in wildlife hunting across the Africa-Europe South-North gradient. PLoS Biol 2022; 20: e3001707. doi: 10.1371/journal.pbio.3001707

6. Robinson HS, Goodrich JM, Miquelle DG, Miller CS, Seryodkin IV. Mortality of Amur tigers: the more things change, the more they stay the same. Integr Zool 2015; 10: 344–53.

7. Nash M, Rafay MF. Craniocervical arterial dissection in children: pathophysiology and management. Pediatr Neurol 2019; 95: 9–18.

8. Liu Y, Li S, Wu Y, et al. The added value of vessel wall MRI in the detection of intraluminal thrombus in patients suspected of craniocervical artery dissection. Aging Dis 2021; 1; 12: 2140–50.

9. Hakimi R, Sivakumar S. Imaging of carotid dissection. Curr Pain Headache Rep 2019;23: e2. doi: 10.1007/s11916-019-0741-9

10. Poledník I, Sulzenko J, Widimsky P. Risk of a coronary event in patients after ischemic stroke or transient ischemic attack. Anatol J Cardiol 2021; 25: 152–5.

11. Murala S, Nagarajan E, Bollu PC. Infectious causes of stroke. J Stroke Cerebrovasc Dis 2022; 31: e106274. doi: 10.1016/j.jstrokecerebrovasdis.2021.106274.

12. Patabendige A, Singh A, Jenkins S, Sen J, Chen R. Astrocyte Activation in neurovascular damage and repair following schaemic stroke. Int J Mol Sci 2021; 22: e4280. doi: 10.3390/ijms22084280.

13. Clark M, Unnam S, Ghosh S. A carotid and vertebral artery dissection review. Br J Hosp Med 2022; 83:1–11.

14. Xia H, Wu Y, Zhao J, et al. The aberrant cross-talk of epithelium-macrophages via METTL3-regulated extracellular vesicle miR-93 in smoking-induced emphysema. Cell Biol Toxicol. 2022; 38: 167–83.

15. Broekx S, Houben R, Stockx L, et al. The external carotid artery as a rare feeder of a spinal dural arteriovenous fistula causing cervical myelopathy: a literature review. Brain Spine 2021: 28; 1: e100299. doi: 10.1016/j.bas.2021.100299.

16. Morales-Primo AU, Becker I, Zamora-Chimal J. Neutrophil extracellular trap-associated molecules: a review on their immunohistological and inflammatory roles. Int Rev Immunol 2022; 41:253–74. DOI: 10.1080/08830185.2021.1921174.

17. Yao J, Bai T, Yang B, Sun L. The diagnostic value of D-dimer in acute aortic dissection: a meta-analysis. J Cardiothorac Surg 2021; 16: e343. doi: 10.1186/s13019-021-01726-1.

18. Koch V, Biener M, Müller-Hennessen M, et al. Diagnostic performance of D-dimer predicting venous thromboembolism and acute aortic dissection. Eur Heart J Acute Cardiovasc Care 2021; 10: 559–66. doi: 10.1177/2048872620907322.

19. Garner M, Yilmaz U, Behnke S. Spontane Dissektionen der hirnversorgenden Arterien. Radiologe 2021;61: 729–35.

20. Janská K, Bodnár R, Janský P, Vosko M. Intravenous thrombolytic therapy for acute nonarteritic central retinal artery occlusion. A review. Cesk Slov Oftalmol 2022; 78: 101–9.

21. Mendelson SJ, Prabhakaran S. Diagnosis and management of transient ischemic attack and acute ischemic stroke: a review. JAMA 2021 ; 325: 1088–98.

22. Bhatia K, Jain V, Aggarwal D, et al. Dual antiplatelet therapy versus aspirin in patients with stroke or transient ischemic attack: meta-analysis of randomized controlled trials. Stroke 2021; 52: e217–e23. doi: 10.1161/STROKEAHA.120.033033.

23. Hogan DF. Feline cardiogenic arterial thromboembolism: prevention and herapy. Vet Clin North Am Small Anim Pract 2017; 47: 1065–82.

24. Rosati LM, Vezzetti A, Redd KT, et al. Early anticoagulation or antiplatelet therapy is critical in craniocervical artery dissection: results from the COMPASS registry. Cerebrovasc Dis 2020; 49: 369–74.

25. Lo ST, Walker AL, Georges CJ, Li RH, Stern JA. Dual therapy with clopidogrel and rivaroxaban in cats with thromboembolic disease. J Feline Med Surg. 2022; 24: 277–83.

26. Birkbeck R, Humm K, Cortellini S. A review of hyperfibrinolysis in cats and dogs. J Small Anim Pract 2019; 60: 641–55.

27. Saw J, Humphries K, Aymong E, et al. Spontaneous coronary artery dissection: clinical outcomes and risk of recurrence. J Am Coll Cardiol 2017; 70: 1148–58.

28. Xu D, Wu Y, Li J, et al. Retrospective comparative analysis of clinical and imaging features of craniocervical artery dissection: spontaneous CAD vs. minor traumatic CAD. Front Neurol 2022; 13: e836997. doi: 10.3389/fneur.2022.836997.

29. Vezzetti A, Rosati LM, Lowe FJ, et al. Stenting as a treatment for craniocervical artery dissection: improved paramount adverse cardiovascular event-free survival. Catheter Cardiovasc Interv 2022; 99: 134–9.

30. Chen Y, Liao K, Ai L, et al. Bacteremia caused by *Bergeyella zoohelcum* in an infective endocarditis patient: case report and review of the literature. BMC Infect Dis 2017; 17: e271. doi: 10.1186/s12879-017-2391-z.

31. Muramatsu Y, Haraya N, Horie K, et al. *Bergeyella zoohelcum* isolated from oral cavities of therapy dogs. Zoonoses Public Health. 2019; 66: 936–42.

32. Lorenzo de Arriba M, Lopez-Serrano S, Galofre-Mila N, Aragon V. Characterisation of Bergeyella spp. isolated from the nasal cavities of piglets. Vet J 2018; 234: 1–6.

33. Yi J, Humphries R, Doerr L, Jerris RC, Westblade LF. *Bergeyella zoohelcum* associated with abscess and cellulitis after a dog bite. Pediatr Infect Dis J 2016; 35: 214–6.

34. Sharma S, Salazar H, Sharma S, Nasser MF, Dahdouh M. *Bergeyella zoohelcum* bacteremia from therapy dog kisses. Cureus 2019; 11: e4494. doi:10.7759/cureus.4494.

35. Zamora L, Domínguez L, Fernández-Garayzábal JF, Vela AI. Bergeyella porcorum sp. nov., isolated from pigs. Syst Appl Microbiol 2016; 39: 160–3.

36. Tomida J, Fujiwara N, Naka T, et al. Spodiobacter cordis gen. nov. sp. nov., a member of the family Flavobacteriaceae isolated from patients with infective endocarditis. Microbiol Immunol 2019; 63: 111–8.

37. Goldstein EJC, Citron DM, Tyrrell KL, Leoncio ES. In vitro activity of Pexiganan and 10 comparator antimicrobials against 234 isolates, including 93 Pasteurella Species and 50 anaerobic bacterial isolates recovered from animal bite wounds. Antimicrob Agents Chemother 2017; 61: e00246-17. doi: 10.1128/AAC.00246-17.

38. Harsent R, Macleod J, Rowlands RS, Smith PM, Rushmere N, Blaxland J. The identification of multidrug-resistant microorganisms, including *Bergeyella zoohelcum*, acquired from the skin/prosthetic interface of amputees and their susceptibility to Medihoney™ and garlic extract (Allicin). Microorganisms 2022 ; 10: e299. doi: 10.3390/microorganisms10020299.

39. Krumbeck JA, Reiter AM, Pohl JC, et al. Characterization of oral microbiota in cats: novel insights on the potential role of fungi in feline chronic gingivostomatitis. Pathogens 2021; 10: e904. doi: 10.3390/pathogens10070904.

40. Fajardo C, Martín C, Costa G, et al. Assessing the role of polyethene microplastics as a vector for organic pollutants in soil: ecotoxicological and molecular approaches. Chemosphere 2022; 288: e132460. doi: 10.1016/j.chemosphere.2021.132460.

41. Proverbio D, Perego R, Baggiani L, Ravasio G, Giambellini D, Spada E. Hematological and biochemical reference values in healthy captive tigers (Panthera tigris). Animals (Basel) 2021; 11: e3440. doi: 10.3390/ani11123440.

Klinične in diagnostične slikovne ugotovitve pri bengalskem tigru (*Panthera tigris tigris*) z disekcijo kraniocervikalne arterije: Poročilo o primeru

P. M. Zadeh, N. Shadan, S. Mohammadi, F. Najafi, A. Bashiri

Izvleček: Namen te študije je bil preučiti različne vidike disekcij kraniocervikalnih arterij, ki so po zaporedju patoloških dogodkov povzročile smrt živali. Po fizičnih poškodbah vratu samice sibirskega tigra, ki so bile posledica agonističnega vedenje samca tigra, smo opravili diagnostične teste, ki so vključevali popolni zdravniški pregled, slikanje MRA s časom leta (TOF) in radiografijo. Vzeli smo tudi vzorce za klinično oceno, hematologijo, mikrobiološko kulturo in antibiogram. Predpisali smo začetno zdravljenje in izvedli PCR. Na žalost so bili ukrepi zdravljenja neustrezni in žival je poginila. Zato smo opravili nekropsijo, histopatološki pregled in imunohistokemično barvanje. Rezultati mikrobiološke preiskave so vključevali prvo identifikacijo bakterije Bergeyella zoohelcum pri tej vrsti živali. Diagnostične ugotovitve na podlagi nekropsije in histoloških preiskav so vključevale anevrizmo, subarahnoidalno krvavitev, ishemično kap ter Hornerjev intramuralni hematom, rupturo karotidnih arterij in notranje jugularne vene, kar še ni bilo opisano. Računalniška tomografija celotnega telesa s prilagojenim protokolom slikanja kraniocervikalnih žil je varna, hitra in izvedljiva metoda za odkrivanje poškodb žil. Ta metoda bi lahko bila del širšega presejalnega protokola za kraniocervikalne žile pri dokumentiranih poškodbah glave in vratu ter mehanizmih poškodb, ki vplivajo tudi na kraniocervikalno področje.

Ključne besede: *Bergeyella zoohelcum*; ishemična kap; subarahnoidalna krvavitev; tiger; prehodni ishemični napad